Author Query Form

Journal Title **:** Journal of Thermoplastic Composite Materials (JTC)
Article Number **:** 390154

Dear Author/Editor,
Greetings, and thank you for publishing with SAGE. Your article has been copyedited and typeset, please return any proof corrections at your earliest convenience. Thank you for your time and effort.

Please ensure that you have obtained and enclosed all necessary permissions for the reproduction of artistic works, (e.g. illustrations, photographs, charts, maps, other visual material, etc.) not owned by yourself, and ensure that the Contribution contains no unlawful statements and does not infringe any rights of others, and agree to indemnify the Publisher, SAGE Publications Ltd, against any claims in respect of the above warranties and that you agree that the Conditions of Publication form part of the Publishing Agreement.

Any colour figures have been incorporated for the on-line version only. Colour printing in the journal must be arranged with the Production Editor, please refer to the figure colour policy outlined in the e-mail.

Erosive Wear Studies of Glass fiber- and Carbon Fiber-reinforced Polyetheretherketone Composites at Low Particle Speed

NEJAT Y. SARI,[1,*] TAMER SINMAZCELIK[1,2] AND TANER YILMAZ[1]

[1]*Department of Mechanical Engineering, Kocaeli University 41040 Kocaeli, Turkey*

[2]*TUBITAK-MRC, Materials Institute, PO Box 21, Gebze, Turkey*

ABSTRACT: In this study, solid particle erosive wear behavior of randomly oriented short glass fiber and carbon fiber-reinforced polyetheretherketone (PEEK) composites was investigated. The solid particle erosion experiments were carried out at six different contact angles (15–90°) and at low particle speed using brown fused aluminum oxide (Al_2O_3) particles (500–710 μm) as an erodent. The PEEK composites showed semi-ductile erosion behavior, with a maximum wear amount at a contact angle of 45°. The fiber type and the contact angle had a significant influence on erosion behavior. Glass fiber-reinforced PEEK composites showed better erosive wear resistance than carbon fibre-reinforced composites. Scanning electron microscopy studies were conducted to understand the wear mechanisms involved during the erosive wear.

KEY WORDS: erosive wear, short fiber composites, polyetheretherketone composites, scanning electron microscopy.

INTRODUCTION

SOLID PARTICLE EROSION is a dynamic process which causes material removal from a target surface due to impingement of fast moving solid particles [1]. Solid particle erosion reveals negative results such as wear of

*Author to whom correspondence should be addressed. E-mail: nsari@kocaeli.edu.tr

0892-7057/10/00 1–18 $10.00/0 DOI: 10.1177/0892705710390154
© The Author(s), 2010. Reprints and permissions:
sagepub.co.uk/journalsPermissions.nav

+ [Ver: A3B2 8.07r/W] [9.11.2010–7:06pm] [1–18] [Page No. 1] FIRST PROOFS {SAGE}JTC/JTC 390154.3d (jtc) Paper: JTC 390154 Keyword

components, surface roughening, surface degradation, macroscopic scooping appearance, and reduction in functional life of the structure. Hence, solid particle erosion has been considered as a serious problem as it is responsible for many failures in engineering applications [2]. Polymer composite materials are finding increased application under conditions in which they may be subjected to solid particle erosion at applications such as pipe lines carrying sand slurries in petroleum refining, helicopter rotor blades, pump impeller blades, high-speed vehicles, and aircrafts operating in desert environments [3]. Erosion resistance of polymer composites which are used in many applications has become an important material property, particularly in the selection of alternative materials [4]. Hence, it becomes imperative to study solid particle erosive wear behavior of polymeric engineering materials in various operating conditions [5]. However, it has been observed that polymer composite materials present a rather poor erosion resistance compared to metallic materials [3]. It is also known that erosive wear of polymer composites is usually higher than that of the unreinforced polymer matrix [3,4,6].

Many researchers have evaluated the wear resistance of polymer composites to various wear conditions such as abrasive [7], erosive [2–6, 8–29], and adhesive wear [30,31]. In the solid particle erosion process of polymers and their composites investigated by many researchers, parameters like fiber and filler type, particle and fabric content, fiber orientation, fiber length, impingement angle, impact velocity, erodent mass flow, erodent size, and the interfacial bonding between fiber and matrix have good influence on the erosion behavior. The influence of these parameters is very strong and any changes in them can markedly affect the rate of material loss. The most important parameters for designs with composites are the fiber/filler content and different types of fiber used for reinforcement in polymers as they control the mechanical and thermo-mechanical properties. In order to obtain the desired material characteristics for a particular application, it is important to know how the composite wear performance changes with the parameters. Polymers and their composites that have been studied include polyetherimide (PEI) [2,12,13,15,21,22], polyetheretherketone (PEEK) [3,25,26,28,29], epoxy [4,6,8,10,14], polyamide (PA) [5,20], polyproplyene (PP) [9], polyurethane (PUR) [11], polyphenylenesulphide (PPS) [16,17,19,23], and polyaryletherketone (PAEK) [18,24,27].

PAEK shows exceptional properties due to its semicrystalline character and the molecular rigidity of its repeating units. PAEKs such as PEEK, polyetherketone (PEK), polyetherketoneketone (PEKK), etc., have similar crystal structures but differ in ketone content [24]. Several investigations have been made on wear behavior of PEEK and its composites. Tewari et al. [3] investigated the solid particle erosion of unidirectional carbon

fiber-reinforced (CF, carbon fiber) PEEK composites. Harsha et al. [18] reported the solid particle erosion behavior of various PAEK composites such as PEEK, PEK, and PEKK at different impingement angles and impact velocities. Voss and Friedrich [25] studied the sliding and abrasive wear behavior of short fiber-reinforced PEEK composites under extremely different types of wear loading . Bahadur and Gong [26] investigated the role of copper compounds as fillers in the friction, transfer, and wear behavior of PEEK using pin-on-disc test rig. Harsha et al. [27] reported the three-body abrasive wear behavior of PAEK composites. Sumer et al. [28] investigated the tribological behavior of PEEK and glass fiber (GF)-reinforced PEEK composites under dry sliding and water-lubricated conditions. Suresh et al. [29] studied the solid particle erosion behavior of neat PEEK matrix and unidirectional GF- and CF-reinforced PEEK and PEKK composites. They ranked the composites in the following sequence characterized by decreasing erosion resistance: CF/PEEK, CF/PEKK, GF/PEKK, and GF/PEEK.

Although a little study has been carried out on erosive wear of PEEK composites, no study has directly compared the different types of random-oriented short fiber reinforcement, i.e., CF and GF on erosive wear behavior of PEEK under low particle speed. In the solid particle erosion process, impact velocities change in the range from 20 to 300 m/s. Inspite of this, specific working conditions involve impact velocities below 20 m/s [32]. The objective of this study was to compare the erosive wear resistance of CF- and GF-reinforced PEEK composites under low particle speed conditions (lower than 20 m/s).

EXPERIMENTAL DETAILS

Material

Random-oriented short GF- and CF-reinforced PEEK composites used in this study were kindly supplied from Victrex as injection molded $80 \times 80\,mm^2$ plaques with thickness of 2 mm. Fiber weight fracture values of the both the composites were 30%. From these molded plaques, test samples, of dimensions approximately $15 \times 80 \times 2\,mm^3$ were cut using a diamond cutter. The details of the composites selected for this study and their fiber contents as well as physical, mechanical, and thermal properties are given in Table 1.

Erosive Wear Studies

A schematic illustration of the low speed solid particle erosion rig used in this study is shown in Figure 1(a). An electric motor drives the system and

Table 1. Material properties (supplier's data).

		Materials	
Property	**Test method**	**PEEK + 30% GF**	**PEEK + 30% CF**
Density (g/cm^3)	ISO 1183	1.51	1.40
Tensile modulus (MPa)	ISO 527-2	11,800	25,000
Tensile stress (Break, MPa)	ISO 527-2	180	240
Tensile strain (break, %)	ISO 527-2	2.7	1.7
Flexural modulus (MPa)	ISO178	11,300	23,000
Flexural strength (MPa)	ISO178	270	350
Compressive stress (MPa)	ISO 604	250	300
Hardness (Shore D)	ISO 868	89	90
Charpy impact strength, unnotched (kJ/m^2)	IS 179/1U	55.00	45.00
Charpy impact strength, notched (kJ/m^2)	ISO 179/1eA	8.00	7.00
Glass transition temperature (°C)	IS 3146	143	143
Melting temperature (°C)	IS 3146	343	343

the speed control unit enables us to adjust desired travel speed of the sample holder in the chamber. Composite specimens were mounted in the sample holder. The chamber was filled up with the erodent. The upper end of the sample was 40 mm beneath the upper erodent particle surface. The composite samples were mounted on the sample holder which could be rotated around the vertical axis. As seen in Figure 1(b), the composite sample follows the circular path into the chamber which has a radius of '*r*.' It is possible to adjust the travel speed by means of changes in '*r*' values in the chamber. Maximum available travel speed can be achieved as 1.57 m/s in this chamber. The contact angle varies between the 15° and 90° with increments of 15°. The angle of contact is enabled to be set in the desired angle. Contact angle is a very important parameter, which affects the erosive wear behavior of the samples remarkably.

Test rig includes a chamber which is filled with erodent particles. In this study, sharp and angular brown fused aluminum oxide (Al_2O_3) was used as erodent. In erosive wear experiments, various erodent particles such as aluminum oxide, silica sand, and silicon carbide can be used. Hardness of brown fused aluminum oxide is higher than that of silica sand, but its hardness is lower than that of silicon carbide. Besides, its density is higher than that of silica sand but lower than that of silicon carbide, namely, aluminum oxide depicts an intermediate property between silica sand and silicon carbide. Therefore, aluminum oxide was preferred as the erodent particles in this study. Sharp, angular aluminum oxide particles with a size of 500–710 μm and a hardness of 9 Moh were selected as the erodent in order

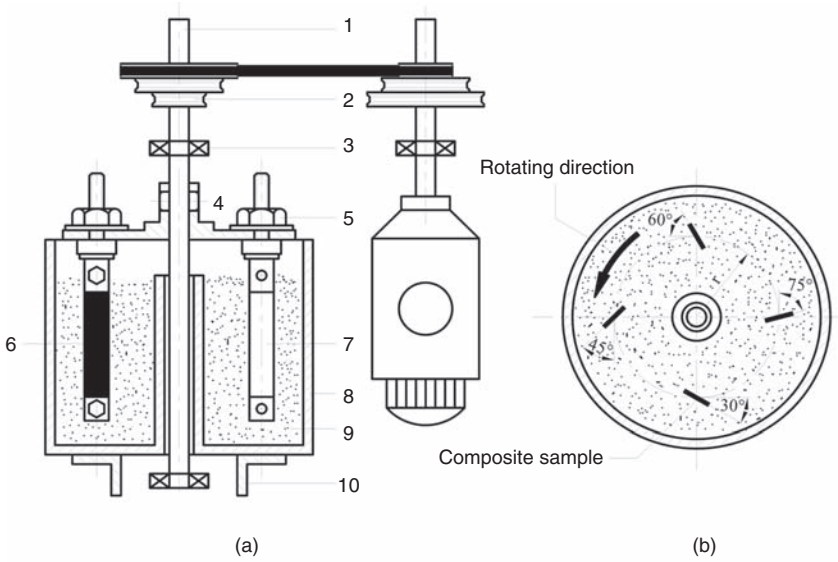

Part no	Part name	Part no	Part name
1	Shaft	6	Sample
2	Belt pulley	7	Sample holder
3	Bearing	8	Chamber
4	Pin	9	Erodent particles
5	Bolt	10	Structure

Figure 1. *(a) Schematic illustration of erosion test rig and (b) rotating path of the composite sample.*

to examine the effect of fiber type on the erosion resistance of the PEEK composites. Figure 2 shows the micrograph of the erodent.

The properties of the erodent and the experimental parameters under which eroson tests were carried out are given in Table 2. In addition, the chemical composition of aluminum oxide erodent is given in Table 3.

The same test procedure was employed for each sample. The erosion tests were conducted at each contact angle by changing the orientation of the sample with respect to the erodent particles. The samples were mounted on the sample holder at six different contact angles as 15°, 30°, 45°, 60°, 75°, and 90°, as shown in Figure 1(b). Wear rates of the samples were determined using weight loss. The samples were cleaned in acetone, dried in oven at 22°C for 2 h, and weighed to an accuracy of 0.1 mg using an electronic

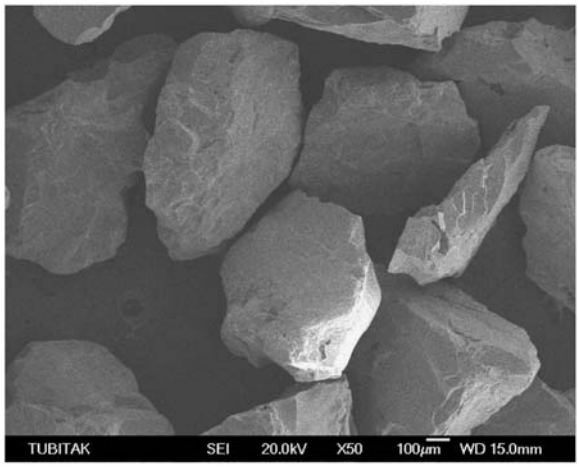

Figure 2. *Scanning electron micrograph of aluminum oxide (500–710 μm).*

Table 2. Properties of erodents used and test parameters.

Erodent	Brown fused aluminum oxide
Erodent size (μm)	500–710
Erodent shape	Angular
Hardness (GPa)	21
Density (g/cm^3)	3.77
Contact angle, α, (°)	15, 30, 45, 60, 75, and 90
Shaft revolution (rpm)	120
Velocity (m/s)	1.57
Test period for each sample (h)	1, 3, 5, and 7
Test temperature	Room temparature

Table 3. Chemical composition of erodent used in erosion tests.

Erodent	Chemical composition
Brown fused aluminum oxide	Al_2O_3, 96%; TiO_2, 2.5%; SiO_2, 0.8%; Fe_2O_3, 0.15%; CaO, 0.21%; and MgO, 0.21%

balance before the wear test. After wear testing, erodent particles which were adhered to the surface of the sample were removed by air blasting. Before samples were weighed at the end of a certain period of erosion test to determine the weight loss, they were cleaned in acetone and dried in oven at 22°C for 2 h so that they were freed of all erodent particles or other foreign substance such as dust, dirt, etc. Great care was given to ensure clean surface before and after wear tests. All erosion tests were performed at

room temperature. Five tests were performed on each parameter and an average value calculated. In erosive wear experiments, samples were separately subjected to erosive wear in the test rig at certain contact angles for 1, 3, 5, and 7 h. Since each sample was not succesively subjected to erosive wear, weight loss of each sample which was obtained at the end of a certain period was directly considered as the cumulative wear rate of that sample. Erodent particles were replaced after certain periods in consideration of the fact that their abrasive capability reduces due to the interaction among themselves.

Characterization of Eroded Samples

At the end of erosive wear tests, each eroded surface was examined under JEOL/JSM-6335 F field emission scanning electron microscope (SEM) and photographs of the eroded surfaces of samples were taken. The samples were gold sputtered in order to reduce charging of the surface.

RESULTS AND DISCUSSION

Erosive Wear Behavior

The cumulative weight loss values obtained after erosive wear experiments using aluminum oxide particles having 500–710 μm particle sizes for GF- (Figure 3(a)) and CF- (Figure 3(b)) reinforced PEEK composites are shown in Figure 3. Erosive weight loss shows a strong dependence on contact angle for all samples. It was observed that cumulative weight loss increases proportionally with erosion time for each contact angle. In the literature, it has been reported that ductile polymers and some elastomers show an initial incubation period with mass gain before steady-state erosion rate is established under constant erosion conditions [6,18,33]. However, in this study, an initial mass gain and incubation period were not observed for the PEEK composites under the chosen experimental condition. It was also reported that initial mass gain and incubation period were not observed for PEEK composites under the solid particle erosion conditions [3,18]. As shown in Figure 3, it was obvious that there was no incubation period for all impingement angles (from 15° to 90°) and there was a linear proportion between erosion weight loss and erosion time. This indicates that repeatable steady state wear mode was reached during the experiments. As shown in Figure 3, the maximum weight loss was reached at the contact angles of 45° for both GF- and CF-reinforced PEEK composites. In addition, as shown in Figure 3(a), the contact angle of 60° was found to be the second highest contact angle after the contact angle

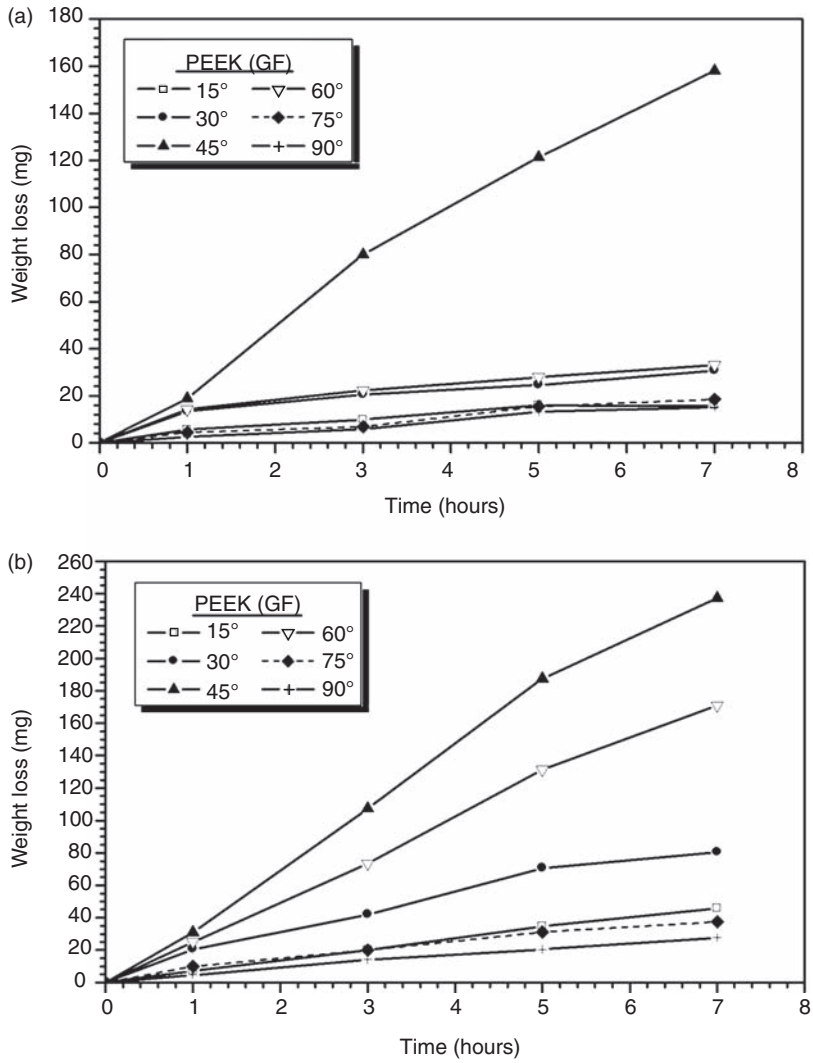

Figure 3. *Cumulative weight loss values of samples as a function of wear time: (a) GF-reinforced PEEK and (b) CF-reinforced PEEK.*

of 45° in GF-reinforced composites. The minimum wear amount among CF-reinforced samples was observed in the sample eroded at the contact angle of 90° (Figure 3(b)). After 7 h of erosion time, the wear amount of GF-reinforced composite eroded at the contact angle of 60° was determined approximately equal to the wear amount of CF-reinforced composite eroded at the contact angle of 90°.

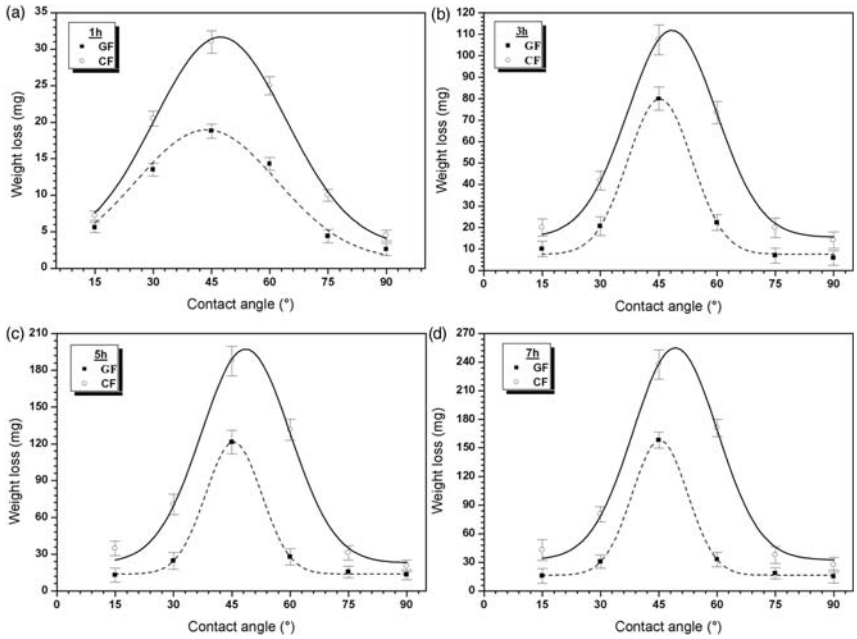

Figure 4. *Weight loss values of the samples as a function of contact angle: (a) 1 h, (b) 3 h, (c) 5 h, and (d) 7 h erosion times.*

Figure 4 shows the influence of the contact angle (α) on the weight loss of GF- and CF-reinforced PEEK composites. The effect of the contact angle on weight loss of the composites is shown in Figure 4(a)–(d) after erosion times of 1, 3, 5, and 7 h, respectively. For both composites, the shapes of the curves are similar at all contact angles. Wear amount is strongly affected by the variation of the contact angle. As shown in Figure 4, both the GF- and CF-reinforced composites exhibited maximum weight loss at the contact angle of 45°. This is an evidence of semi-ductile erosion behavior. Besides, at all contact angles, it is shown that the wear amount of CF-reinforced PEEK composites are higher than those of GF-reinforced PEEK composites. Hence, it can be said that erosion weight loss depends on the type of fiber used in the composite. In the erosion of polymers, thermoplastics exhibit a more ductile response than thermosets [29]. It is known that impingement angle is one of the most important parameters for the erosion behavior of materials. Erosive wear behavior can be grouped in ductile and brittle categories, based on the dependence of their erosion rate on impingement angle. However, this grouping is not definitive, as the erosion behavior of materials strongly depends upon the experimental conditions and composition of target materials [9,18]. The behavior of ductile materials like

polymers is characterized by maximum erosion rate at low impingement angles (15–30°). Brittle materials, on the other hand, show maximum erosion under normal impingement angle (90°). Reinforced composites, have been shown, however, to exhibit a semi-ductile behavior with maximum erosion occuring in the angular range 45–60° [2,6,18]. However, in the literature, mixed trends have been reported even for nominally brittle or ductile materials [18]. PEEK is a relatively ductile matrix. The ductility of the matrix is not reflected with erosion behavior. Also in this study, glass and CFs, which are typical brittle materials, were used as reinforcement for the PEEK matrix.

The dependency of erosion rate of glass and CF-reinforced composites on the impact angle has been reported in the literature by many investigators. In general, many investigators have carried out erosion tests using angular silica sand and silicon carbide (SiC) erodent particles at different impact velocities (25–66 m/s). In this study, the erosive wear tests were performed under low particle speeds using brown fused aluminum oxide erodent particles. Hence, it is difficult to compare present erosion data precisely with the literature data. Tewari et al. [3] reported that maximum erosion rate occurred at the impact angle of 60° for unidirectional CF-reinforced PEEK composites. Harsha and Jha [4] performed erosion tests on unidirectional GF- and CF-reinforced epoxy composites and concluded their erosion behavior as semi-ductile with peak erosion at an impingement angle of 60°. Suresh et al. [29] concluded that unidirectional GF- and CF-reinforced PEEK composites showed maximum erosion at the impact angle of 60°. Miyazaki and Hamao [34] carried out experiments to study the effects of matrix material, impact angle, and particle velocity on the solid particle erosion behavior of short GF- and CF-reinforced PEEK resin. It was reported that PEEK and its composites show maximum erosion rate at a low impact angle of 30°. Zahavi and Schmitt [35] reported that maximum weight loss occurred at the impingement angle of 45–60° for glass epoxy composite. It was concluded that inclusion of brittle fibers in a ductile matrix results in the shift in the peak erosion angle to higher side. However, Rattan and Bijwe [12] observed a ductile response for carbon fabric-reinforced PEI composite.

In general, thermoplastic matrix composites exhibit a ductile erosive wear as a result of plastic deformation, ploughing, and other damage accumulation processes, while thermosetting matrix composites erode in a brittle manner as a result of generation and propagation of surface lateral cracks. However, this failure classification is not definitive because the erosion behavior of composites depends strongly on the experimental conditions and the composition of the target material. It is reported in the literature that when the erosive particles hit the target at oblique angles, the impact

+ [Ver: A3B2 8.07r/W] [9.11.2010-7:06pm] [1-18] [Page No. 10] FIRST PROOFS {SAGE}JTC/JTC 390154.3d (jtc) Paper: JTC 390154 Keyword

force can be divided in two constituents: one tangential (F_t) to surface of the material and the other normal (F_n). F_t controls the abrasive and F_n is responsible for the impact phenomenon. As the impact angle shifts toward 90°, the effects of F_t become marginal. It is obvious in the case of normal impact (90°) that all available energy is dissipated by impact and microcracking, while at oblique angles, due to the decisive role of the F_t, the damage occurs by microcutting and microploughing [15,16,18,32,36].

Surface Morphology of Eroded Surface

SEM micrographs of the worn surfaces of both GF- and CF-reinforced PEEK composites are shown in Figures 5–7. SEM studies of worn surfaces support the involved mechanisms and indicated pulverization of wear debris, wear debris embedment, matrix removal, exposure of fibers, fiber breaking, and detachment of broken fibers from the PEEK matrix. A similar kind of observations was also observed by the other investigators for polymers like PEI, epoxy, and PAEK [2–4,6–8,12,18]. In this study, all the GF-reinforced composites showed less wear amount than CF-reinforced composites. The likely reason of this difference can be attributed to dominant wear mechanisms of the samples. Harsha et al. [18] concluded that the CF reinforced to PAEK matrix had worse erosive wear resistance compared to GF-reinforced PAEK composites. In GF-reinforced composites, most of the GF debris fractured or broke into small pieces due to the impact of erodent particles during erosive wear embedded in the worn matrix. This mechanism results in lower wear amounts in weight loss measurements carried out after the erosive wear experiments. However, in CF-reinforced composites, it was observed that most of the wear debris were detached from the matrix. The SEM micrographs of the worn surfaces of GF- and CF-reinforced composite samples eroded at the contact angle of 30° for 7 h are shown in Figure 5(a)

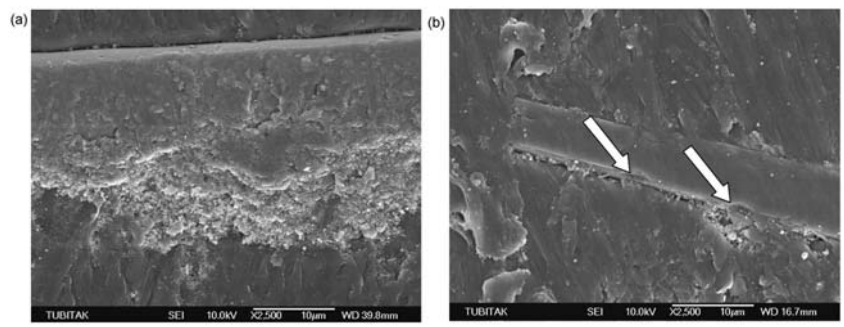

Figure 5. *SEM micrographs of: (a) GF- and(b) CF-reinforced composite surfaces eroded at contact angle of 30° for 7 h.*

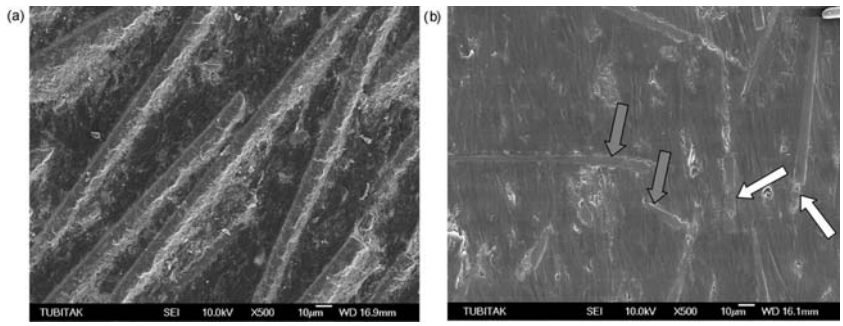

Figure 6. *SEM micrographs of: (a) GF- and (b) CF-reinforced composite surfaces eroded at contact angle of 15° for 7 h.*

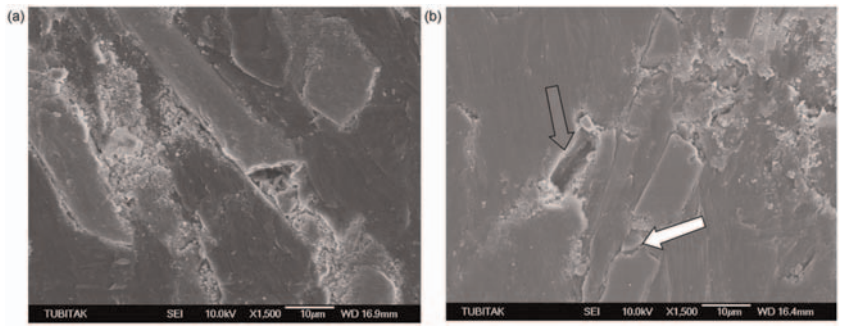

Figure 7. *SEM micrographs of: (a) GF- and (b) CF-reinforced composite surfaces eroded at contact angle of 60° for 7 h.*

and (b), respectively. The fiber debris and the matrix erosion can be clearly seen from the micrograph of GF-reinforced composite in Figure 5(a). The wear debris virtually got collected on the matrix downward in the direction of wear and got adhered to the matrix; they help in reducing further wear of PEEK composite. Also, the fiber fractures in CF-reinforced composite samples along with fiber–matrix debonding and the matrix erosion were observed (Figure 5(b)). In Figure 5(b), the fiber fractures were indicated by the white arrows on the micrograph. A similar kind of observations was also observed for epoxy. Harsha et al. [4] reported that the pulverized wear debris were adhered to the matrix and they helped in reducing further wear of epoxy. They also reported that erosion mechanism of GF-reinforced epoxy composite was characterized by fiber–matrix debonding, brittle fracture of matrix, and pulverization of fibers.

The SEM micrographs of the worn surfaces of GF- and CF-reinforced composite samples eroded at the contact angle of 15° for 7 h are shown in Figure 6(a) and (b), respectively. For the both types of composites, it was

determined that the angle of 15° causes less wear compared to the other angles. No damage of the fibers was observed on the micrograph of GF-reinforced composite eroded at the contact angle of 15° for 7 h. However, it was seen that collection on the right of fibers occurred and wear debris adhered to matrix (Figure 6(a)). In addition, damages such as the fiber breakages, the matrix erosion, the start of fiber–matrix debonding were seen from the microphotographs of CF-reinforced composite in Figure 6(b). In Figure 6(b), the white arrows show the damage on fibers and the hatched arrows show the fiber–matrix debonding.

Figure 7(a) and (b) shows the micrographs of the wear surfaces of GF- and CF-reinforced composites eroded at the contact angle of 60° for 7 h, respectively. The contact angle of 60° is the angle at which the maximum wear amount occurred after the contact angle of 45° for both GF- and CF-reinforced samples. It was seen that fibers in the GF-reinforced composite fractured and broke, but most of them remained in their places in the matrix, and only a small amount of them got detached from the matrix (Figure 7(a)). In CF-reinforced composite (Figure 7(b)), multiple fractures on the fibers in addition to the intense matrix erosion, were observed and it was also seen that some fiber particles remained in the matrix (as indicated by the white arrow on the micrograph). Further damage is characterized by separation and detachment of broken fibers from the PEEK matrix as indicated by the hatched arrow on the micrograph in Figure 7(b). It is genereally accepted that wear behavior of short fiber-reinforced composites is dominated by the process of fiber peeling-off, which typically occurs following such sequential stages: fiber thinning, fiber cracking, and fiber removal [14]. In this study, the fiber peeling-off plays a key role. The exposure of fibers to erosive environment results in a condition where the matrix gets removed as a result of the impact of the erodent particles on the composite surface. The continuous impact of the solid erodent particles during wear causes multiple fractures on fibers and some of the broken fibers remain in the matrix and some leave their place and fiber peeling-off occurs (Figure 7(b)).

Figure 8(a) and (b) show the SEM micrographs of the surfaces of the GF- and CF-reinforced composites eroded at the contact angle of 45° for 3 h, respectively. In the GF-reinforced composite, breakages on fibers (indicated by the white arrows on the micrograph) along with matrix wear were seen, and it was also seen that the broken fiber debris remained in the matrix and that the broken fiber particle tried to detach from the matrix as displayed with the hatched arrow (Figure 8(a)). Figure 8(a) shows the wear surface morphology of the GF-reinforced composite after 3 h of wear time. It is expected that in the ongoing wear time the broken fiber particle (indicated by the hatched arrow on the micrograph) will probably get detached from the matrix due to the effect of continuous impact of the

+ [Ver: A3B2 8.07r/W] [9.11.2010–7:06pm] [1–18] [Page No. 13] FIRST PROOFS {SAGE}JTC/JTC 390154.3d (jtc) Paper: JTC 390154 Keyword

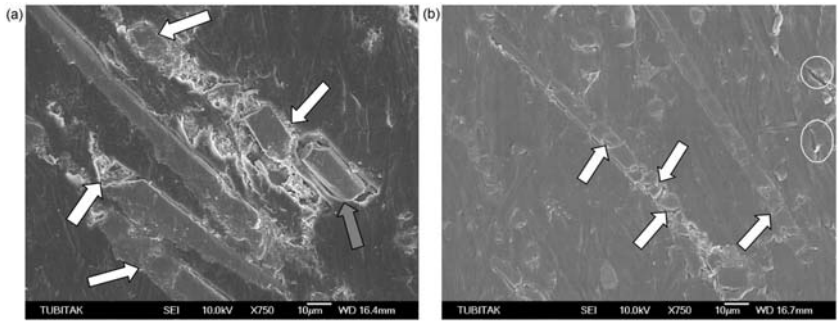

Figure 8. *SEM micrographs of: (a) GF- and (b) CF-reinforced composite surfaces eroded at contact angle of 45° for 3 h.*

erodent particles. Further continuation of erosion by the erodent particle impacts resulted in damage to the interface between the fibers and the resin matrix. This damage was characterized by the separation and detachment of the broken fibers from the matrix [10]. The behavior of this damage can be attributed to the following mechanism. It is well known that the fibers in composites subjected to particle flow break on bending [37]. In case of an impact having a parallel component of velocity with respect to the fiber orientation, bending requires particle indentation into the composites. The indentation involves compressive stresses and resistance to microbending is high. Thus, there is a local removal of resin material from the impacted surface, which results in the exposure of the fibers. Transverse particle impact resistance to lateral component of the bending moment is lower and bundles of fibers get bent and broken easily. Also, in the case of transverse erosion, high interfacial tensile stresses are generated by particle impacts. This causes intensive debonding and breakage of the fibers, which are not supported by the matrix [6,10]. From the micrograph of the CF-reinforced composite in Figure 8(b), it is seen that many multiple fractures on fibers occurred as indicated by the white arrows and that deep wear traces existed as indicated by circles. The detachment from the matrix of fiber particles broken into many small pieces will be much easier.

The worn surfaces of GF- and CF-reinforced composites eroded at the contact angle of 45° for 7 h are shown in Figure 9(a) and (b), respectively. As stated before, the contact angle of 45° is the angle at which the maximum erosion occurred in both composites. The deep wear traces, fiber–matrix debonding, and wear debris occurred as a result of the damage in the fibrers, which can be clearly seen from the micrograph of the GF-reinforced composite in Figure 9(a). Also, it is seen that most of the fiber debris do not leave the matrix. On the micrograph in Figure 9(a), the fibers damaged as wear debris in the matrix on their places are indicated by the white arrows

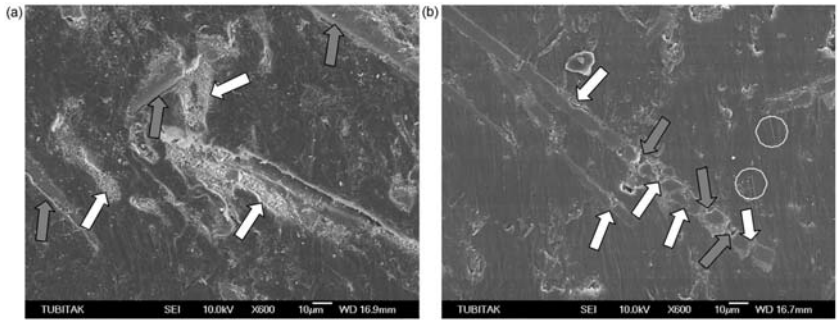

Figure 9. *SEM micrographs of: (a) GF- and (b) CF-reinforced composite surfaces eroded at contact angle of 45° for 7 h.*

and fiber–matrix debonding is indicated by the hatched arrows. In Figure 9, from SEM observations of eroded surfaces, it appears that composites under consideration exhibit several stages of the erosion and material process. First, there is local removal of the resin material from the impacted surface, which results in exposure of the fibers to the erosive environment. Also, solid erodent particles impact on the fibers and cause the fibers to break owing to the formation of cracks perpendicular to their length. These cracks across the fiber are caused by bending due to the impact of these particles on the unsupported fibers. Bending is possible because the matrix resin surrounding and supporting the fibers have been removed [8,10]. From the micrograph of the CF-reinforced composite (Figure 9(b)), many multiple fractures (indicated by the white arrows) and cavities on the matrix occurred due to the detachment of the broken fiber particles from the matrix (indicated by the hatched arrows) are seen. Also, from the micrograph of the same sample, deep grooves, which indicate the material removal by microploughing wear mechanism, as indicated by the circles, are seen. Arjula et al. [21] reported that maximum erosion occurred as a result of damage features like microcracking of fibers and plastic deformation of matrix for unidirectional CF-reinforced PEI composite.

CONCLUSIONS

Based on this study of the solid particle erosion of random-oriented short GF- and CF-reinforced PEEK composites at various contact angles and low particle speeds, the following conclusions are drawn:

1. The influence of the contact angle on erosive wear of both composites exhibited semi-ductile erosive wear behavior with a maximum wear at the contact angle of 45°.

2. The fiber type has a significant influence on the weight loss of composites. The weight loss of CF-reinforced composites is higher than that of GF-reinforced composites. Therefore, observed difference in erosive behavior of these composites should be attributed to different fibers and wear mechanisms.
3. In GF-reinforced composites, the pulverized wear debris is adhered to the matrix and helps in reducing further wear of GF-reinforced PEEK composite. This effect is responsible for the low wear rate of GF-reinforced PEEK composites as compared to the CF-reinforced PEEK composites.
4. SEM studies of worn surfaces support the involved wear mechanisms and indicated pulverization of wear debris, wear debris embeddement, matrix removal, exposure of fibers, fiber breaking, and detachment of broken fibers from the PEEK matrix.

REFERENCES

1. Arjula, S. and Harsha, A.P. (2006). Study of Erosion of Polymers and Polymer Composites, *Polymer Testing*, **25**: 188–196.
2. Harsha, A.P. and Thakre, A.A. (2007). Investigation on Solid Particle Erosion Behaviour of Polyetherimide and its Composites, *Wear*, **262**: 807–818.
3. Tewari, U.S., Harsha, A.P., Häger A.M. and Friedrich, K. (2002). Solid Particle Erosion of Unidirectional Carbon Fibre Reinforced Polyetheretherketone Composites, *Wear*, **252**: 992–1000.
4. Harsha, A.P. and Jha, S.K. (2008). Erosive Wear Studies of Epoxy-based Composites at Normal Incidence, *Wear*, **265**: 1129–1135.
5. Rajesh, J.J., Bijwe J., Tewari, U.S. and Venkataraman, B. (2001). Erosive Wear Behavior of Various Polyamides, *Wear*, **249**: 702–714.
6. Tewari, U.S., Harsha, A.P., Häger, A.M. and Friedrich, K. (2003). Solid Particle Erosion of Carbon Fibre– and Glass Fibre–Epoxy Composites, *Composites Science and Technology*, **63**: 549–557.
7. Jalham, I.S. (2005). The Influence of Process and Material Variables on the Surface Properties of Polystyrene Matrix Reinforced with Silica Sand, *Journal of Thermoplastic Composite Materials*, **18**: 529–541.
8. Srivastava, V.K. and Pawar, A.G. (2006). Solid Particle Erosion of Glass Fibre Reinforced Flyash Filled Epoxy Resin Composite, *Composites Science and Technology*, **66**: 3021–3028.
9. Barkoula, N.M. and Kocsis, J.K. (2002). Effects of Fibre Content and Relative Fibre-orientation on the Solid Particle Erosion of GF/PP Composites, *Wear*, **252**: 80–87.
10. Srivastava, V.K. (2006). Effects of Wheat Starch on Erosive Wear of E-glass Fibre Reinforced Epoxy Resin Composite Materials, *Materials Science and Engineering A*, **435–436**: 282–287.
11. Zhou, R., Lu, D.H., Jiang, Y.H. and Li, Q.N. (2005). Mechanical Properties and Erosion Wear Resistance of Polyurethane Matrix Composites, *Wear*, **259**: 676–683.
12. Rattan, R. and Bijwe, J. (2007). Influence of Impingement Angle on Solid Particle Erosion of Carbon Fabric Reinforced Polyetherimide Composite, *Wear*, **262**: 568–574.

+ [Ver: A3B2 8.07r/W] [9.11.2010–7:06pm] [1–18] [Page No. 16] FIRST PROOFS {SAGE}JTC/JTC 390154.3d (jtc) Paper: JTC 390154 Keyword

13. Bijwe, J. and Rattan, R. (2007). Influence of Weave of Carbon Fabric in Polyetherimide Composites in Various Wear Situations, *Wear*, **263**: 984–991.
14. Zhang, H., Zhang, Z. and Friedrich, K. (2007). Effect of Fiber Length on the Wear Resistance of Short Carbon Fiber Reinforced Epoxy Composites, *Composites Science and Technology*, **67**: 222–230.
15. Sarı, N. and Sınmazçelik, T. (2007). Erosive Wear Behaviour of Carbon Fibre/ Polyetherimide Composites under Low Particle Speed, *Materials and Design*, **28**: 351–355.
16. Sınmazçelik, T. and Taşkıran, İ. (2007). Erosive Wear Behaviour of Polyphenylenesulphide (PPS) Composites, *Materials and Design*, **28**: 2471–2477.
17. Arjula, S., Harsha, A.P. and Ghosh, M.K. (2009). Solid Particle Erosion Studies on Polyphenylene Sulfide Composites and Prediction on Erosion Data Using Artificial Neural Networks, *Wear*, **266**: 184–193.
18. Harsha, A.P., Tewari, U.S. and Venkataraman, B. (2003). Solid Particle Erosion Behaviour of Various Polyaryletherketone Composites, *Wear*, **254**: 693–712.
19. Ahmed, T.J., Nino, G.F., Bersee, H.E.N. and Beukers, A. (2009). Improving Erosion Resistance of Polymer Reinforced Composites, *Journal of Thermoplastic Composite Materials*, **22**: 703–725.
20. Rajesh, J.J., Bijwe, J., Venkataraman, B. and Tewari, U.S. (2004). Effect of Impinging Velocity on the Erosive Wear Behaviour of Polyamides, *Tribology International*, **37**: 219–226.
21. Arjula, S., Harsha, A.P. and Ghosh, M.K. (2008). Erosive Wear of Unidirectional Carbon Fibre Reinforced Polyetherimide Composite, *Materials Letters*, **62**: 3246–3249.
22. Rattan, R. and Bijwe, J. (2006). Carbon Fabric Reinforced Polyetherimide Composites: Influence of Weave of Fabric and Processing Parameters on Performance Properties and Erosive Wear, *Materials Science and Engineering A*, **420**: 342–350.
23. Sari, N.Y. (2009). Influence of Erodent Particle Types on Solid Particle Erosion of Polyphenylene Sulphide Composite under Low Particle Speed, *Polymer Composites*, **30**: 1442–1449.
24. Harsha, A.P. and Tewari, U.S. (2002). Tribo Performance of Polyaryletherketone Composites, *Polymer Testing*, **21**: 697–709.
25. Voss, H. and Friedrich, K. (1987). On the Wear Behaviour of Short-Fibre-Reinforced Peek Composites, *Wear*, **116**: 1–18.
26. Bahadur, S. and Gong, D. (1987). The Role of Copper compounds as Fillers in the Transfer and Wear Behavior of Polyetheretherketone, *Wear*, **154**: 151–165.
27. Harsha, A.P., Tewari, U.S. and Venkataraman, B. (2003). Three-Body Abrasive Wear Behaviour of Polyaryletherketone Composites, *Wear*, **254**: 680–692.
28. Sumer, M., Unal, H. and Mimaroglu, A. (2008). Evaluation of Tribological Behaviour of PEEK and Glass Fibre Reinforced PEEK Composite under Dry Sliding and Water Lubricated Conditions, *Wear*, **265**: 1061–1065.
29. Suresh, A., Harsha, A.P. and Ghosh, M.K. (2009). Solid Particle Erosion of Unidirectional Fibre Reinforced Thermoplastic Composites, *Wear*, **267**: 1516–1524.
30. Viña, J., García, M.A., Castrillo, M.A., Viña, I. and Argüelles, A. (2008). Wear Behavior of a Glass Fiber-reinforced PEI Composite, *Journal of Thermoplastic Composite Materials*, **21**: 279–286.
31. Li J. and Xia, Y.C. (2010). The Friction and Wear Properties of Thermoplastic PA6 Composites Filled with Carbon Fiber, *Journal of Thermoplastic Composite Materials*, **23**: 337–349.
32. Chacon-Nava, J.G., Stott, F.H., De La Torre, S.D. and Martínez-Villafañe, A. (2002). The Friction and Wear Properties of Thermoplastic PA6 Composites Filled with Carbon Fiber, *Materials Letters*, **55**: 269–273.
33. Li, J. and Hutchings, I.M. (1990). Resistance of Cast Polyurethane Elastomers to Solid Particle Erosion, *Wear*, **135**: 293–303.

+ [Ver: A3B2 8.07r/W] [9.11.2010–7:06pm] [1–18] [Page No. 17] FIRST PROOFS {SAGE}JTC/JTC 390154.3d (jtc) Paper: JTC 390154 Keyword

34. Miyazaki, N. and Hamao, T. (1994). Solid Particle Erosion of Thermoplastic Resins Reinforced by Short Fibers, *Journal of Composite Materials*, **28**: 871–883.
35. Zahavi, J. and Schmitt Jr, G.F. (1981). Solid Particle Erosion of Reinforced Composite Materials, *Wear*, **71**: 179–190.
36. Wang, Y.Q., Huang, L.P., Liu, W.L. and Li, J. (1998). The Blast Erosion Behaviour of Ultrahigh Molecular Weight Polyethylene, *Wear*, **218**: 128–133.
37. Pool, K.V., Dharan, C.K.H. and Finnie, I. (1986). Erosive Wear of Composite Materials, *Wear*, **107**: 1–12.

+ [Ver: A3B2 8.07r/W] [9.11.2010-7:06pm] [1-18] [Page No. 18] FIRST PROOFS {SAGE}JTC/JTC 390154.3d (jtc) Paper: JTC 390154 Keyword